Coatings with Columnar Microstructures for Thermal Barrier Applications

Georg Mauer* and Robert Vaßen

Columnar-structured thermal barrier coatings (TBCs) manufactured by electron beam-physical vapor deposition (EB-PVD) are well known to exhibit high strain tolerance. However, as EB-PVD is a high-vacuum process, it is expensive. Suspension plasma spraying (SPS) and plasma spray-physical vapor deposition (PS-PVD) are alternatives for the manufacture of similar microstructures. Herein, the state of the art of manufacturing columnar-structured TBCs by SPS and PS-PVD is outlined. Both processes have been investigated and further developed at Forschungszentrum Jülich for many years. The mechanisms leading to the formation of columnar-structured coatings are described and differentiated from EB-PVD. Examples are given for SPS and PS-PVD columnar microstructures and their life performance.

1. Introduction

Thermal barrier coating (TBC) systems have been applied for several decades to improve the performance of modern gas turbine aeroengines, shipboard engines, and land-based industrial gas turbine engines. On the one hand, TBCs can reduce the temperature of the metallic substrate, which results in improved component durability. On the other hand, an increase in efficiency can be achieved by permitting higher turbine inlet temperatures even beyond the prevailing critical values implied by the limited capabilities of single-crystal nickel-based superalloys even in combination with sophisticated cooling concepts.^[1]

TBC systems are complex, multilayered, and multimaterial systems. ^[2] They consist of at least two layers, a metallic bond coat layer and an insulating ceramic topcoat. ^[3] The bond coat provides oxidation resistance for the base material and adherence of the coating. The topcoat is for heat insulation as it shows low

Dr. G. Mauer, Prof. R. Vaßen Forschungszentrum Jülich GmbH, Institute of Energy and Climate Research (IEK) Jülich 52428, Germany E-mail: g.mauer@fz-juelich.de

The ORCID identification number(s) for the author(s) of this article can be found under https://doi.org/10.1002/adem.201900988.

© 2019 The Authors. Published by WILEY-VCH Verlag GmbH & Co. KGaA, Weinheim. This is an open access article under the terms of the Creative Commons Attribution-NonCommercial-NoDerivs License, which permits use and distribution in any medium, provided the original work is properly cited, the use is non-commercial and no modifications or adaptations are made.

DOI: 10.1002/adem.201900988

thermal conductivity resulting from material characteristics as well as from the microstructure.^[4]

Two methods of deposition techniques have become well established for ceramic TBC topcoats, electron beam-physical vapor deposition (EB-PVD)^[5] on the one hand and atmospheric plasma spraying (APS)^[6] on the other hand, which is based on the deposition of numerous liquid splats. Coatings manufactured by EB-PVD are mainly used for highly thermomechanically loaded blades of aeroengines.^[7] Due to their specific columnar microstructures, they show high in-plane strain tolerance. However, in the vertical direction, the thermal conductivity is relatively high.

The APS process meanwhile displays operational robustness and economic viability; hence more TBCs are now being developed with this method. In contrast to EB-PVD coatings, the pores and voids are mainly in-plane oriented. This is favorable for the achievement of low thermal conductivities in the vertical direction. However, APS coatings often show spallation due to the strain energy that is stored during thermal cycling processes.

One approach to reduce stress accumulation in APS coatings is to achieve low-stiffness microstructures by intersplat microcracks and intrasplat pores. $^{[9]}$ Another possibility is the introduction of so-called vertical segmentation cracks with a length of at least half of the coating thickness. $^{[10]}$ With optimized plasmaspraying conditions and powder feedstock, segmented yttriastabilized zirconia (YSZ) TBCs with a thickness of 500 μm and segmentation crack densities above 8 mm $^{-1}$ were successfully produced. As the porosity of such coatings was smaller compared to standard porous ones, a higher thermal conductivity had to be accepted. Nevertheless, these coatings showed good performance in thermal cycling tests due to their increased strain tolerance. $^{[11]}$

The logical continuation of this approach is the generation of EB-PVD-like columnar structures also in plasma-sprayed ceramic topcoatings. This was one major motivation to develop the suspension plasma spraying (SPS) process^[12] and plasma spray-physical vapor deposition (PS-PVD).^[13] **Table 1** summarizes the mentioned preparation methods for TBCs, the corresponding feedstock varieties, and the basic types of microstructures that can be obtained.

For many years, SPS and PS-PVD have been intensively developed at Forschungszentrum Jülich. One major focus is the application of these processes to manufacture TBCs. In addition, there have been strong concerted activities for the development of new

www.aem-journal.com



Table 1. Summary of the mentioned preparation methods for TBCs.

Process			Feedstock	Microstructure
EB-PVD			Solid ingot	Compact columns with intercolumnar gaps
Thermal spraying	APS	Conventional	Powder, typical particle diameter $10-150\mu m$	Lamellar, in-plane oriented voids and pores; with adapted powder and spray parameters: dense vertically cracked
		SPS	Suspension, typical particle diameter ${<}1\mu m$	Porous vertically cracked; with adapted powder and spray parameters: porous columns with intercolumnar gaps
	PS-PVD		Powder, typical particle diameter 5–20 μm	With adapted powder and spray parameters: porous columns with intercolumnar gaps

TBC materials as well as in performance testing of TBC systems under realistic conditions.[14]

In this work, the state of the art of manufacturing columnarstructured ceramic TBC topcoats is outlined. The mechanisms leading to the formation of columnar-structured coatings by SPS and PS-PVD are described and differentiated from EB-PVD. Examples of microstructures and life performance are given for SPS and PS-PVD columnar coatings. In fact, this article is intended to be a review, however, not in a more general sense because it focuses on Forschungszentrum Jülich's work on producing columnar-structured TBCs. The context with extant research activities and another technology is established by referring to the corresponding publications.

2. Formation Mechanisms of Columnar-**Structured Coatings**

In EB-PVD, the formation mechanisms of columnar microstructures are fundamentally different from those in SPS and PS-PVD. They are described in the following sections for the sake of completeness, although Forschungszentrum Jülich does not have any own EB-PVD activities in the TBC area.

2.1. Electron Beam-Physical Vapor Deposition

EB-PVD is a method of physical vapor deposition in which feedstock material in a crucible is converted from solid to vapor by a high-energy electron beam in a vacuum chamber. The electrons are generated in a high-voltage gun by a charged tungsten filament and accelerated toward the crucible, which is connected to a power source and acts as an anode. The evaporated feedstock atoms or molecules condense on the surfaces in the vacuum chamber that are within line of sight, forming a thin layer. The thickness and homogeneity of the coating can be controlled by adjusting the power, diameter, and position of the electron beam. In addition, the substrate can be heated. During deposition, the sample fixture keeps rotating to get a stable substrate temperature and uniform coating thickness. [15]

EB-PVD coatings have a relatively homogeneous columnar structure composed of compact single columns. Figure 1 shows a typical example. Three characteristic microstructural features can be distinguished:^[17] 1) columns and intercolumnar gaps originating from macroscopic shadowing and rotation of the substrate. 2) Globular and elongated rounded pores are a consequence of rotation. [18] They are assumed to be mostly closed.

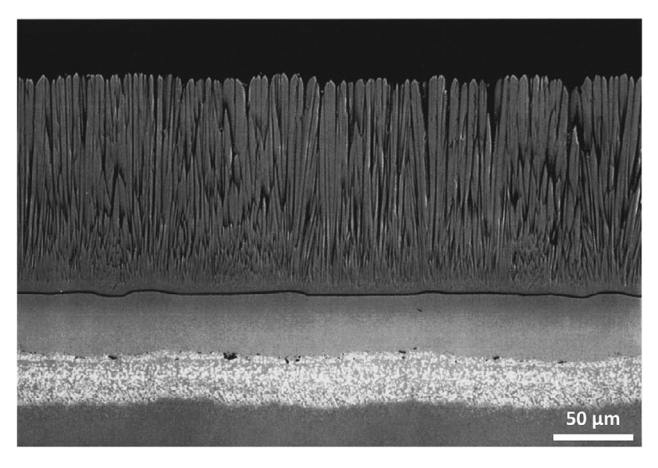


Figure 1. Example of a columnar-structured TBC deposited by EB-PVD. Reproduced with permission. [16] Copyright 1996, AIP Publishing.

3) The third type, referred to as "feather arms," is a consequence of shadowing by growth steps on the column tips near the center of a column.[19]

The intercolumnar gaps contribute mainly to the strain tolerance of the TBCs, whereas lower thermal conductivities of EB-PVD TBCs rely mainly on types 2 and 3 intracolumnar porosity; type 1 intercolumnar gaps are less effective in this regard. [20]

The typical facetted tops of the columns indicate that preferential growth directions exist as the atoms/molecules can diffuse after absorption on the surface to preference low-energy sites. Several studies have been conducted to find relationships between crystallographic textures and processing conditions. The most important parameters are the substrate temperature, the vapor incidence angle, the chamber pressure, and the deposition rate. [21] For YSZ, a fiber texture of (111) was observed at substrate temperatures lower than 900 °C. In contrast, a preferred orientation of (200) was dominant above 900 °C. Columnar grains were observed to exhibit predominantly <100> orientation. The vapor incidence angle and the substrate rotation can also affect the texture. Hence, other planes such as (110), (311), and (211) were found as well. $^{[22]}$

The main advantage of columnar microstructures manufactured by EB-PVD is the tolerance against tensile stresses, erosion, and thermal shock resulting from the segmentation of the coatings by the intercolumnar gaps and the compactness of the column's microstructure, respectively.

2.2. Suspension Plasma Spraying

SPS is an emerging plasma-spray technology, in which the powder feedstock is dispersed in a liquid suspension that is injected into the plasma jet. Finely grained feedstock powders smaller than $\approx\!10\,\mu m$ cannot be processed in dry state because they are not sufficiently flowable. Hence, the powder flux is unsteady or even interrupted by clogging. In contrast, the use of suspensions yields a higher flexibility as feedstock particles even in the sub-micrometer range can be processed. After injection, the suspension droplets break up in the plasma jet, and the particles form small agglomerates which are melted and accelerated. Impinging on the substrate, small splats are formed with a diameter of a few hundred nanometers to a few micrometers. Thus, they are significantly smaller compared with conventional APS. [24]

The plasma jet impacts the substrate and forms an adherent boundary layer. If the spray direction is more or less perpendicular to the substrate surface, the flow stagnates near the point of impact and is deflected in the direction parallel to the substrate surface. This is also dependent on the overall substrate shape (e.g., flat or cylindrical).^[25] Anyhow, the plasma gas encounters substantial changes of flow velocities and directions close to the substrate.^[26]

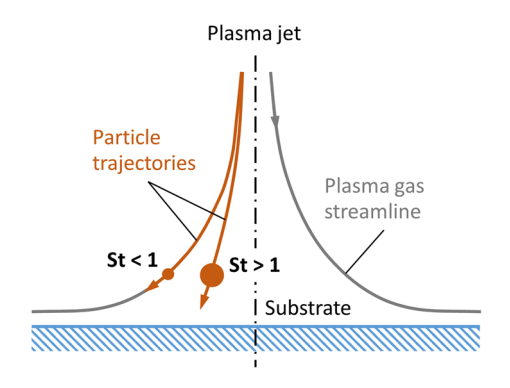


Figure 2. Schematic illustration of the development of particle trajectories in an axisymmetric plasma jet normal to a flat substrate, principal cases of St < 1 and St > 1.

If the characteristic time for momentum transfer from fluid to particles, τ_p , is significantly larger than the characteristic time of the direction change of the flow, τ_g , particles are prone to detach from the flow due to their inertia. In the reverse case, particle trajectories and fluid streamlines are virtually coincident and particles follow the fluid narrowly. τ_p depends on the particle density and diameter as well as on the viscosity of the gas, whereas τ_g is a function of the streamline's local curvature and velocity. The ratio of these characteristic times constitutes the dimensionless Stokes number $St=\tau_p/\tau_g$. The two principal cases of St<1 and St>1 are schematically shown in Figure 2.

Stokes numbers were calculated for typical SPS conditions.^[27] The results show that for smaller particles ($d < 1 \mu m$) close to the substrate, Stokes numbers are subcritical (St < 1), as shown in Figure 3a. This means that the particle trajectories are almost coincident with the streamlines of the fluid, as also found in the simulations of Jadidi et al.^[28] If the spray distance is increased from 60 to 100 mm, a further decrease in the Stokes numbers is observed (Figure 3b) because the particle relaxation times, $\tau_{\rm p}$, remain virtually unchanged, whereas the characteristic times for the directional change of the flow, $\tau_{\rm g}$, rise. The governing parameters are mentioned earlier. The same trend was observed by Jadidi et al.[29] for suspension high-velocity flame spraying (S-HVOF); however, it was more pronounced. To sum up, it is likely that small particles under SPS conditions can either create defects as they tend to impact on the sides of surface protrusions or are carried away by the gas and thus do not contribute to the coating deposition. In the following sections, it is described how such kind of defects can be the nuclei to initiate stacking errors and columnar growth.

Van Every et al.^[30] characterized the effect of different relations of drag and inertial forces as a function of the particle size. However, it would have been more precise to refer to the Stokes numbers.

Depositing smallest particles, plasma drag forces dominate the particle inertia and redirect the velocity from normal to parallel to the surface; particles impact on the sides of asperities. These are either roughness peaks or irregularly distributed single splats on the substrate surface, referred to as "roots." At further deposition, the coating grows competitively as smaller protrusions are shaded by larger ones. This results in the

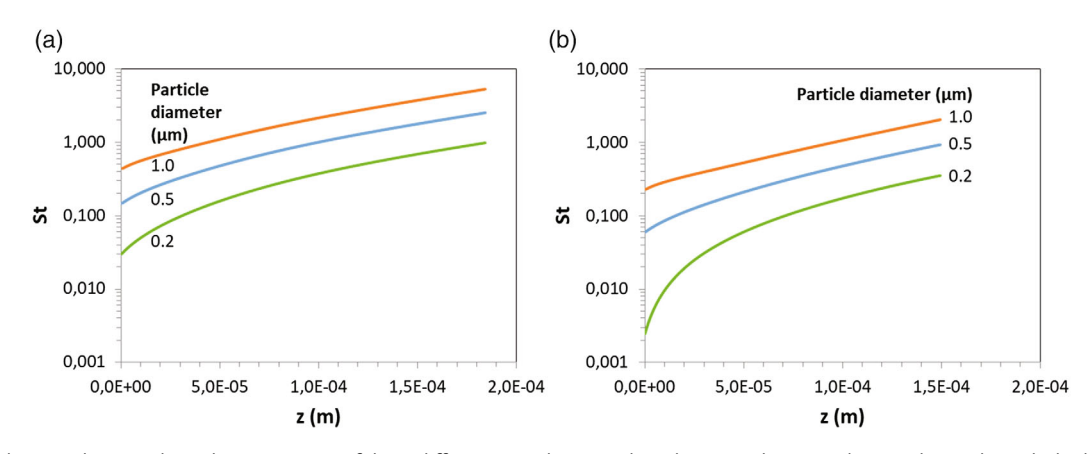


Figure 3. Stokes numbers St along the trajectories of three different particle sizes plotted against the normal z coordinate through the boundary layer (substrate surface at z = 0); a) 60 mm spray distance (Reproduced with permission. [27] Copyright 2019, Springer Nature) and b) 100 mm spray distance.

velocity.

www.advancedsciencenews.com

formation of typical conically shaped columns. For larger particles, the velocity is predominantly directed normally, but parallel components still affect the deposition; convergent porosity bands between surface asperities can be created. Beyond a specific particle diameter, plasma drag forces virtually do not affect particle trajectories and the microstructural evolution. Hence, a uniform coating is obtained leveling the surface profile. This particular particle size depends on the substrate roughness and on particular plasma parameters such as temperature, pressure, and

Bernard et al.^[32] illustrated the formation of typical tapered columns by the concurrence of small and large particles by the scheme shown in **Figure 4**. The schematic also reveals that the scale of the substrate surface asperities must be large with respect to the diameter of the impacting particles; otherwise, these roots are quickly evened. In SPS, the particle size is mainly determined by the particle size and solid load in the suspension as well as by the injection conditions.

Seshadri et al.^[33] designed a process map on the basis of spray experiments. Different microstructure evolution zones were identified at different torch operating conditions considering also the effects of suspension fragmentation in the plume and different melting regimes. In addition, the substrate roughness was found to have a strong impact on the column morphology.

Likewise, Racek^[34] described the formation of large columnar stacking defects if the substrate surface roughness is significantly higher than the average diameter of the impacting particles. Increasing the surface roughness intensifies the accumulation of deposited particles on asperity sides and thus column formation. On smooth surfaces, however, the column sizes and their dimensions become more dispersed.^[35] This can affect the strain tolerance negatively as the intercolumnar gaps that can open and provide stress relaxation are less distinct.^[32]

To conclude, a small ratio of splat size to asperity size favors column formation. Such an effect can be used to tailor microstructures of SPS coatings from dense vertically cracked to columnar structures.^[36] This is illustrated by the examples shown in **Figure 5**. The coatings shown were sprayed with the Axial III torch (Northwest Mettech Corp.), a torch allowing the axial injection of the feedstock materials. This type of injection has certain advantages for SPS coatings as it leads to a rather complete penetration of the droplets into the plasma plume.

2.3. Plasma Spray-Physical Vapor Deposition

To prevent oxidation, for a long time already, bond coats are deposited by plasma spraying under a protective argon atmosphere and low pressure (<10 kPa; low pressure plasma spraying, LPPS). Several years ago, the pressure was decreased (<500 Pa) to obtain particular thin and dense coatings. This process is termed "very low plasma spraying (VLPPS)."[37] It was developed further, increasing electrical currents up to 3 kA so that an input power level of 150 kW and more was achieved. If appropriate parameters and powders are applied, it is even possible to evaporate feedstock material. This particular process is termed "plasma spray physical vapor deposition (PS-PVD)."[13] Computational fluid dynamic simulations for a typical PS-PVD process to deposit columnar YSZ revealed that 64% of the plasma net power was absorbed by the feedstock particles and 57% of the feedstock mass flow was transferred to vapor.[38]

Evaporated feedstock atoms and molecules are suspended by the plasma gas and follow the streamlines. In the boundary layer of the substrate, supersaturation is likely so that stable clusters can be formed. However, they are very small as they grow from small nuclei only during the short time interval, and they travel through the boundary layer. Thus, it can be expected that such clusters also follow the gas streamlines closely even under PS-PVD conditions, which are characterized by very low plasma densities and thus pronounced noncontinuum effects.^[27]

As molecules and clusters are diverted parallel to the substrate surface, columns are generated by shadowing due to the interaction between surface roughness and angular directions of arriving particles. This shadowing intensifies as the coating grows. Thus, the microstructure shows typical tapered columns with a featherlike inner structure and domed tops, separated by voids, as shown in **Figure 6**. This formation mechanism is principally similar to SPS albeit molecules and clusters are deposited in PS-PVD, whereas in SPS the coating is built up from impacting small liquid droplets.

The similarity of the formation mechanisms is confirmed by Monte Carlo simulations conducted by Wang et al.^[40] It is demonstrated that the shape, inclination, and porosity of the columns are significantly determined by the distribution of the particle impact angles. **Figure 7** shows some typical results. The broader the distribution of the vapor incident angles, the more pronounced

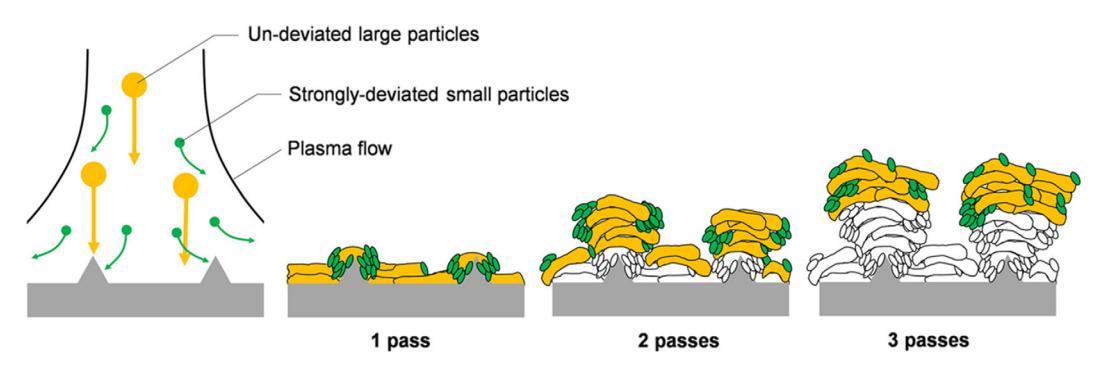


Figure 4. Schematic representation of the formation of typical tapered columns by the concurrence of small and large particles in SPS. Reproduced with permission. [32] Copyright 2017, Springer Nature.

www.advancedsciencenews.com



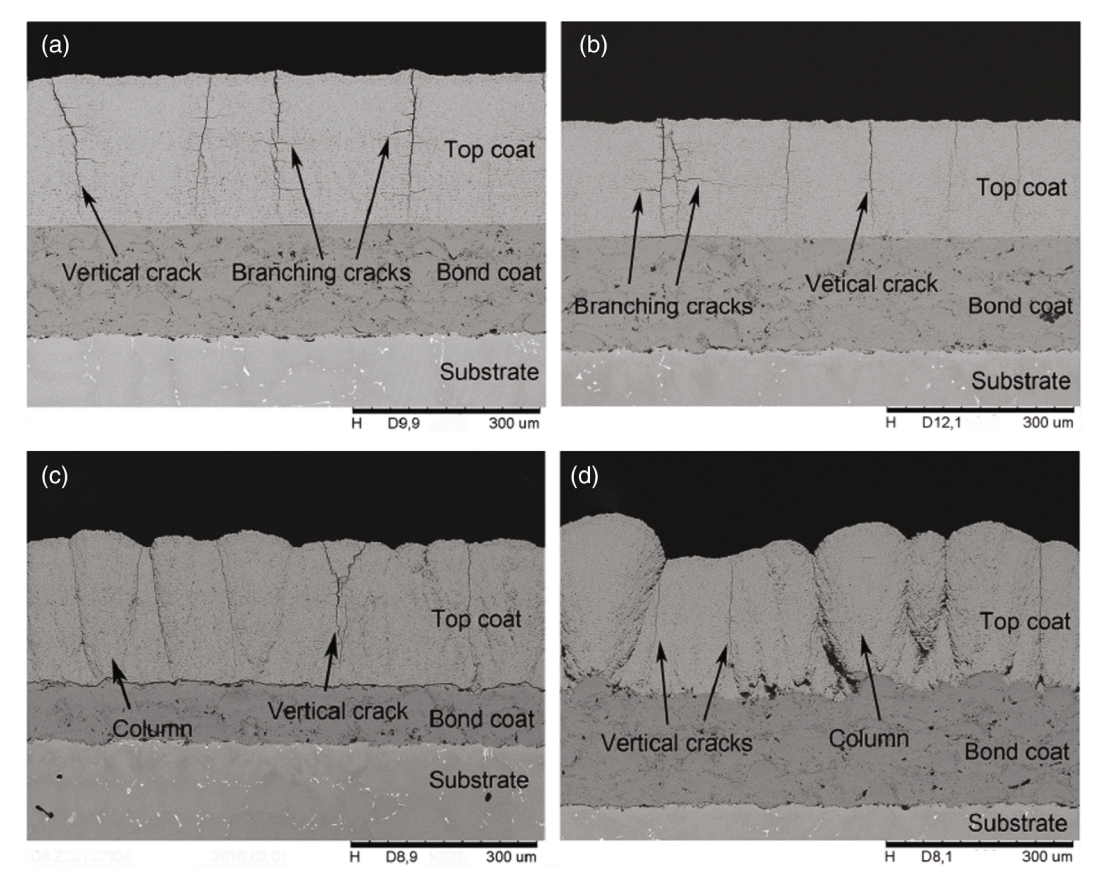


Figure 5. Cross-sectional scanning electron microscope (SEM) images of as-sprayed YSZ topcoats deposited by SPS on bond-coated substrates with different surface treatments: a) mirror polishing, b) grinding, c) grit blasting, and d) as-sprayed. Reproduced with permission.^[39] Copyright 2017, MDPI.

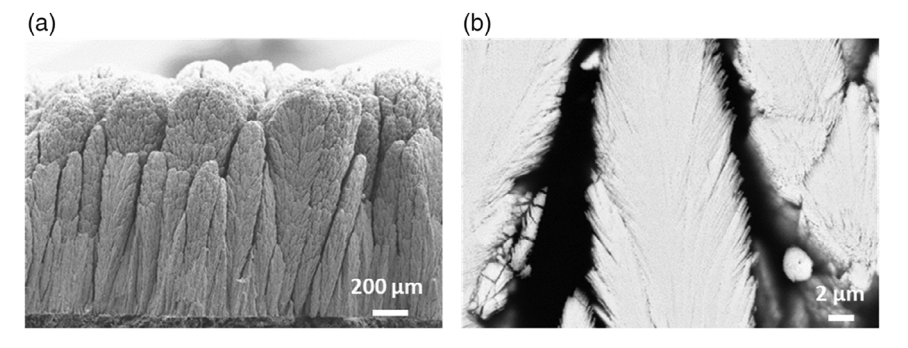


Figure 6. SEM images of columnar YSZ microstructures deposited by PS-PVD. a) Fracture surface of the coating and b) cross section of single columns. Reproduced with permission.^[41] Copyright 2013, Springer Nature.

is the shape of the columns. These findings were obtained with regard to the PS-PVD process, but are principally valid for other spray processes like SPS, where the feedstock particles are sufficiently small, so they are diverted by the plasma gas stream in a parallel direction to the substrate surface when they approach it. Thus, the distribution of incident angles is broadened.

Figure 8 shows the electron backscatter diffraction (EBSD) results of a YSZ columnar-structured TBC deposited by PS-PVD. [42] The image quality map (Figure 8a) shows that viable diffraction patterns were obtained which could be well resolved.

Although X-ray diffraction (XRD) analyses exhibited tetragonal lattice symmetry, the orientations determined by EBSD given in the orientation map (Figure 8b) were indexed with reference to the cubic system because the patterns appeared symmetric within the resolution of the imaging system. Initially, the coating consists of small and randomly orientated equiaxed crystalline grains. Similarly, this was also found in EB-PVD coatings where the first lamina (about 0.1 μm thick) exhibits equiaxed grains of $\approx\!30\,nm$ diameter. $^{[43]}$ Subsequently, with increasing coating thickness, the grains grow as large columns with specific crystal



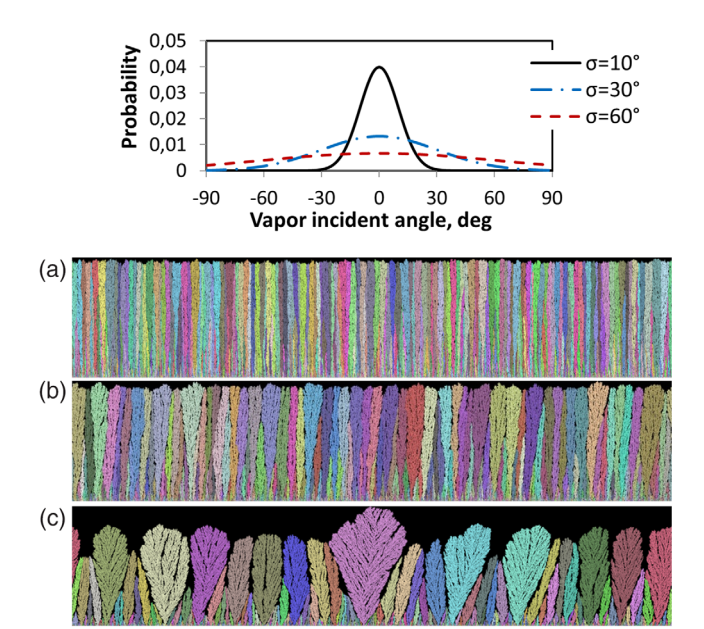


Figure 7. Monte Carlo simulation of the formation of typical columnar microstructures for different distributions (the colors represent individual columns); the standard deviation of the vapor incident angle is a) 10°, b) 30°, and c) 60°. Reproduced with permission. [40] Copyright 2018, Elsevier.

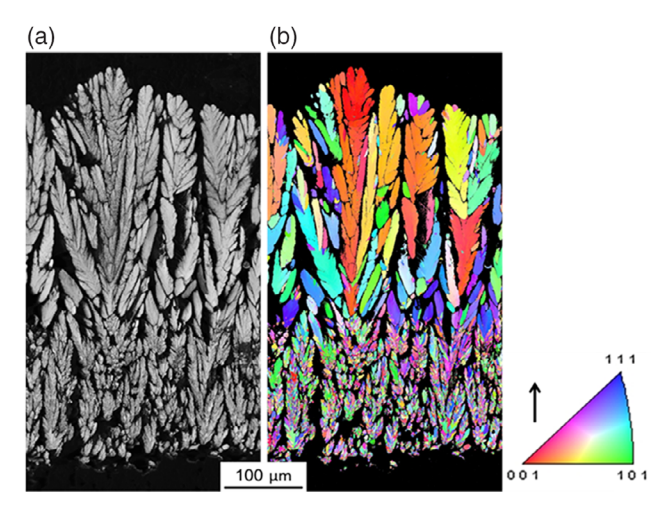


Figure 8. EBSD analysis of an YSZ columnar-structured TBC deposited by PS-PVD. a) Image quality map and b) orientation map. Reproduced with permission. [42] Copyright 2018, Elsevier.

orientations. This is a clear indication that molecules and small clusters were deposited mainly from the vapor phase. As different columns have individual orientations, the overall coating appears to be randomly orientated. This was principally confirmed also by transmission electron microscope (TEM) analyses and is obviously the reason why no crystallographic textures could be found by XRD. [44] Thus, PS-PVD columnar structures are just apparently polycrystalline while this is actually true for SPS coatings that are formed from many fast-solidifying liquid splats.

3. Life Performance of Columnar-Structured TBCs

As mentioned earlier, Forschungszentrum Jülich is not active in EB-PVD of TBCs. Thus, life performance results are given here only for columnar-structured TBCs deposited by SPS and PS-PVD and examined in Jülich. As experimental lifetimes are highly dependent on the way of testing, no external lifetime data of EB-PVD coatings was considered for comparison.

3.1. Suspension Plasma-Sprayed Coatings

Columnar microstructures made by SPS have been tested in gradient rig tests in Jülich as a close to service test bed. Cycling was stopped when an obvious delamination (with an area larger than 25 mm²) occurred on the disk-shaped IN738 superalloy samples (30 mm in diameter). More details on the setup of the burner rig facility were given by Traeger et al. [45] In these tests, the microstructure of the coatings and by that the mechanical properties such as Young's modulus and fracture toughness have been varied in a rather wide range. At first, the stability of the microstructure during thermal treatment has been investigated.^[46] As expected, sintering takes place and leads to an increase in Young's modulus and fracture toughness within the columns. Important for the application is that the column gaps are not closed but even further opened due to the sintering. So it is expected that the strain tolerance of the coating should remain.

Looking at the SPS coatings with different microstructures and hence mechanical properties, the lifetime of these coatings could be described by a subcritical crack growth law. Lifetime divided by the defect size in the as-sprayed condition was plotted against the toughness of the material divided by the actual stress intensity, **Figure 9**. The figure shows a linear dependence which indicates a power law with an exponent of 3.5.

The optimization of the coating microstructure, i.e., low Young's modulus combined with high toughness, could improve

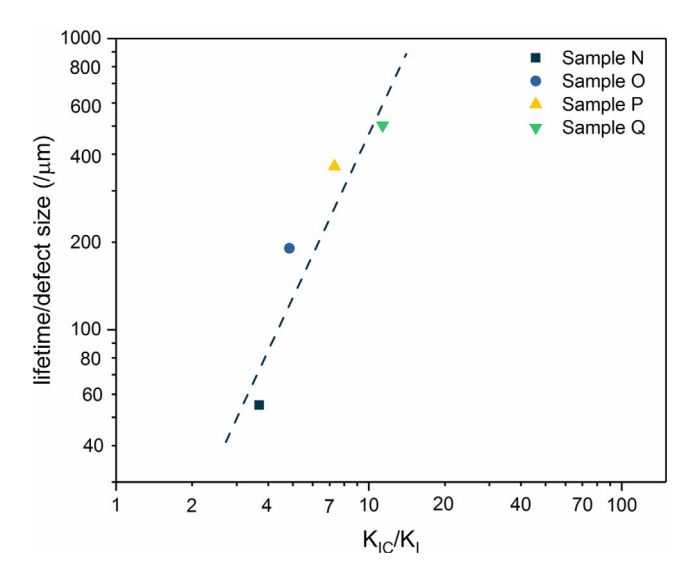


Figure 9. Lifetime divided by the initial defect size as a function of critical to apparent stress intensity factor (Reproduced with permission.^[39,48] Copyright 2017, MPDI; Copyright 2019, Forschungszentrum Jülich).

www.aem-journal.com

the performance of the SPS system; however, a comparison with standard APS coatings still revealed a reduced lifetime. New strategies have been developed to further improve the performance. One very effective way is the use of thin intermediate APS layer underneath the SPS topcoat. [47] With this approach, TBC systems with a higher lifetime than APS systems could be obtained. Improved lifetimes compared with APS systems could also be demonstrated for YSZ/Gd₂Zr₂O₇ double layer systems. In Figure 10, an SEM micrograph of a double layer coating after burner rig test is shown, indicating that failure occurs very late after rather complete β-phase depletion of the bond coat. In addition to their excellent burner rig performance, optimized multilayered systems also show an improved resistance against calcium, magnesium, aluminum, and silicon oxide (CMAS) attack, which is a severe issue, especially for aeroengines (e.g., in the form of volcanic ash).^[49]

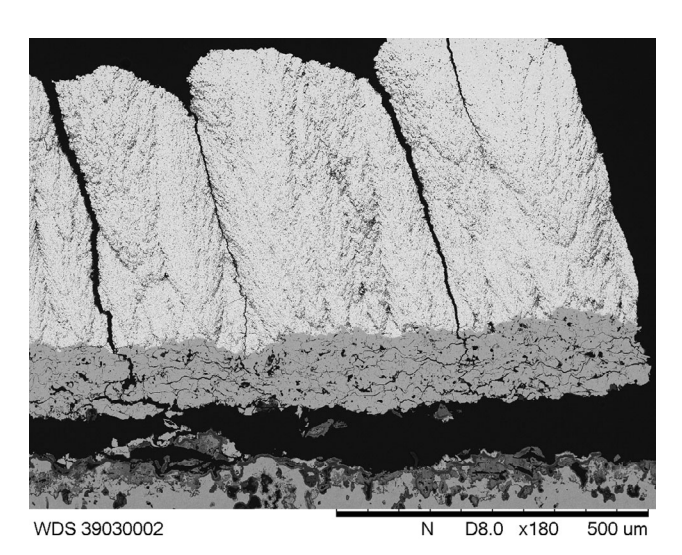


Figure 10. SEM micrograph of a GZO/YSZ double layer after test in burner rig with rather complete β-phase depletion of the bond coat. Reproduced with permission. [49] Copyright 2019, Wiley.

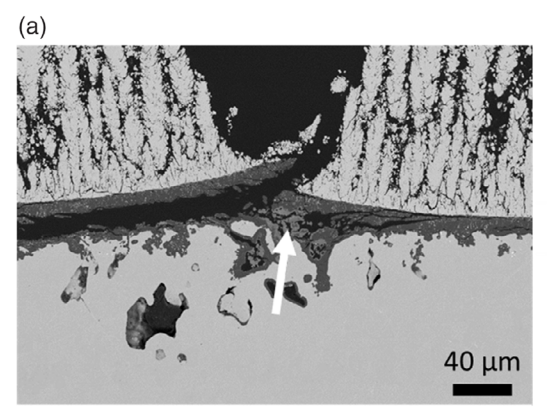
3.2. Plasma Spray-Physical Vapor Deposited Coatings

The failure analysis of a TBC system with an YSZ topcoat deposited by PS-PVD after cyclic thermal gradient test is shown in Figure 11. Details of the experimental setup and procedure can be found in the study by Traeger et al. [45] The test conditions are specified in the caption.

During thermal cycling, a thermally grown oxide (TGO) layer consisting of compact alumina is generally formed at the interface of bond coat and ceramic topcoat. On PS-PVD samples, the latter was locally bulged and highly deformed. However, failures within the ceramic TBC were not observed indicating a high strain tolerance. For conventional TBCs deposited by APS, such failure mode is unusual. The bulges result from the nonuniform fast growth of transient oxides (Cr2O3, spinel (Co,Ni)Cr₂O₄) later.^[50] This is initiated by the pronounced depletion of the aluminum-rich β-phase in the bond coat so that the aluminum diffusion toward the TGO is tied off. Obviously. the durability of the columnar-structured topcoat exceeded the service capability of the bond coat. Compared with standard APS coatings, the lifetime was improved by factor of larger than two.[50]

Because of their open porosity, it is an obvious question whether columnar TBC microstructures are more susceptible to erosive and high-temperature corrosive attack than conventional APS coatings. In aeroengines and land-based gas turbines, dust, sand, volcanic ash, and runway debris are ingested with the intake air. In addition to mechanical degradation by erosion, such contaminants can cause a special form of corrosion attack. Their main constituents are glass-forming oxides of calcium, magnesium, aluminum, and silicon (CMAS). At temperatures above 1200 °C, these contaminants melt, adhere to the surface, and can penetrate the TBC. Due to the chemical interaction and the volume expansion at crystallization, TBCs may be severely degraded and lose their protective function. [52]

The erosion resistance of columnar PS-PVD coatings was found to be lower compared with that of conventional APS coatings. However, this could be significantly increased even beyond that by adjusting the plasma parameter, thus creating a denser



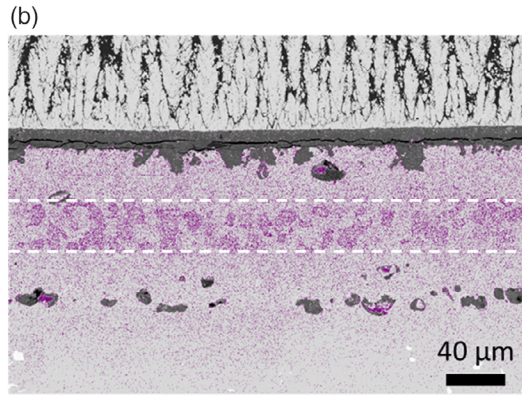


Figure 11. Particular failure mode of a YSZ columnar-structured TBC deposited by PS-PVD, thermal cycling conditions $T_{\text{surface}} = 1382 \,^{\circ}\text{C}$, $T_{
m bondcoat} pprox 1113$ °C, 1185 cycles (pprox 99 h at high temperature). a) Failure due to transient oxide formation (marked by the arrow) and b) eta-phase distribution (contrasted by image editing, the dotted lines demarcate the zones of β -phase depletion). Reproduced with permission. (51) Copyright 2017, IOP Publishing.

www.aem-journal.com

4DVANCED

microstructure. With regard to the stability against CMAS under thermal cycling with temperature gradients, it was found that the lifetimes of TBCs deposited by PS-PVD were comparable to those deposited by EB-PVD or APS. [52]

4. Conclusions

In this work, the basic mechanisms leading to the formation of columnar-structured TBCs in SPS and PS-PVD are outlined. Columns are generated by shadowing due to the interaction between surface asperities and angular directions of arriving particles. The surface asperities are either roughness peaks or irregularly distributed single splats on the substrate surface. In principle, columns are stacking defects that are formed if the scale of the substrate surface asperities is sufficiently large with respect to the average diameter of the impacting particles.

In addition, the specific plasma parameters and the substrate geometry have a considerable impact on the tendency to generate columns as they determine the formation of the streamlines around the part to be coated. The particle acceleration due to directional changes of the plasma flow on the one hand and the particle inertia on the other hand govern the particle impact angle on the substrate.

Life performance tests showed that columnar-structured TBCs have the potential to be superior to conventional APS coatings and even to exceed the service capability of the bond coat. To achieve this, specific measures with respect to the substrate preparation and layer architecture are required.

This research is part of manifold efforts to improve TBCs to come to terms with the growing demands of modern energy technology. [4a,53] Important future research directions, particularly at Forschungszentrum Jülich, will be the improvement of the deposition rates using suspensions with high solid loads and increased powder feed rates in SPS and PS-PVD, respectively. Initial activities on processing topcoat materials other than YSZ, e.g., Gd₂Zr₂O₇, will be continued. Moreover, there is a strong need to adapt and develop process diagnostics to support the improvement of the reliability and robustness of SPS and PS-PVD. Even though optical emission spectroscopy was already successfully applied to characterize the plasma and evaporated feedstock material in these processes, tiny droplets and particles need to be detected under in-flight conditions. The development of corresponding equipment is only at the beginning.

Conflict of Interest

The authors declare no conflict of interest.

Keywords

columnar microstructures, electron beam-physical vapor deposition, plasma spray-physical vapor deposition, suspension plasma spraying, thermal barrier coatings

> Received: August 15, 2019 Revised: October 18, 2019 Published online: December 5, 2019

- [1] D. R. Clarke, M. Oechsner, N. P. Padture, MRS Bull. 2012, 37, 891.
- [2] D. R. Clarke, S. R. Phillpot, Mater. Today 2005, 8, 22.
- [3] N. P. Padture, M. Gell, E. H. Jordan, Science 2002, 296, 280.
- [4] a) R. Vaßen, M. O. Jarligo, T. Steinke, D. E. Mack, D. Stöver, Surf. Coat. Technol. 2010, 205, 938; b) G. Mauer, R. Vaßen, Surf. Eng. 2011, 27, 477; c) G. Mauer, M. O. Jarligo, D. E. Mack, R. Vaßen, J. Therm. Spray Technol. 2013, 22, 646.
- [5] J. Singh, D. E. Wolfe, J. Mater. Sci. 2005, 40, 1.
- [6] a) R. B. Heimann, Plasma Spray Coating: Principles and Applications, Wiley-VCH, Weinheim, Germany 2008: b) L. Pawlowski, The Science and Engineering of Thermal Spray Coatings, Wiley, Chichester, UK 2008; c) P. L. Fauchais, J. V. R. Heberlein, M. I. Boulos, Thermal Spray Fundamentals: From Powder to Part, Springer, New York 2014.
- [7] A. Feuerstein, J. Knapp, T. Taylor, A. Ashary, A. Bolcavage, N. Hitchman, J. Therm. Spray Technol. 2008, 17, 199.
- [8] H. Echsler, D. Renusch, M. Schütze, Mater. Sci. Technol. 2004, 20, 307.
- [9] a) M. Ahrens, R. Vaßen, D. Stöver, S. Lampenscherf, J. Therm. Spray Technol. 2004, 13, 432; b) G. Mauer, R. Vaßen, D. Stöver, Surf. Coat. Technol. 2009, 204, 172.
- [10] P. Bengtsson, T. Ericsson, J. Wigren, J. Therm. Spray Technol. 1998, 7, 340.
- [11] M. Karger, R. Vaßen, D. Stöver, Surf. Coat. Technol. 2011, 206, 16.
- [12] a) A. Killinger, R. Gadow, G. Mauer, A. Guignard, R. Vaßen, D. Stöver, J. Therm. Spray Technol. 2011, 20, 677; b) P. Fauchais, M. Vardelle, A. Vardelle, S. Goutier, J. Therm. Spray Technol. 2015, 24, 1120.
- [13] a) K. von Niessen, M. Gindrat, A. Refke, J. Therm. Spray Technol. 2010, 19, 502; b) K. von Niessen, M. Gindrat, J. Therm. Spray Technol. 2011, 20. 736.
- [14] G. Mauer, Therm. Spray Bull. 2013, 6, 86.
- [15] a) U. Schulz, S. G. Terry, C. G. Levi, Mater. Sci. Eng., A 2003, 360, 319; b) D. Zhang, in Thermal Barrier Coatings (Eds: H. Xu, H. Guo), Woodhead Publishing, Oxford 2011, p. 3.
- [16] R. J. Christensen, D. M. Lipkin, D. R. Clarke, K. Murphy, Appl. Phys. Lett. 1996, 69, 3754.
- [17] U. Schulz, B. Saruhan, K. Fritscher, C. Leyens, Int. J. Appl. Ceram. Technol. 2004, 1, 302.
- [18] O. Unal, T. E. Mitchell, A. H. Heuer, J. Am. Ceram. Soc. 1994, 77, 984.
- [19] S. G. Terry, J. R. Litty, C. G. Levi, in Elevated Temperature Coatings: Science and Technology, Vol. 3 (Ed: J. M. Hampikian), TMS, Warrendale, PA 1999, p. 13.
- [20] A. A. Kulkarni, H. Herman, J. Almer, U. Lienert, D. Haeffner, J. Ilavsky, S. Fang, P. Lawton, J. Am. Ceram. Soc. 2004, 87, 268.
- [21] W. He, Deposition Mechanisms of Thermal Barrier Coatings (TBCs) Manufactured by Plasma Spray-Physical Vapor Deposition (PS-PVD), Forschungszentrum, Zentralbibliothek, Jülich, Germany 2017.
- [22] Y. H. Sohn, R. R. Biederman, R. D. Sisson, Thin Solid Films 1994, 250, 1.
- [23] H. Kassner, R. Siegert, D. Hathiramani, R. Vassen, D. Stoever, J. Therm. Spray Technol. 2008, 17, 115.
- [24] R. Vaßen, H. Kaßner, G. Mauer, D. Stöver, J. Therm. Spray Technol. 2010, 19, 219.
- [25] K. Pourang, C. Moreau, A. Dolatabadi, J. Therm. Spray Technol. 2016,
- [26] B. Selvan, K. Ramachandran, B. C. Pillai, D. Subhakar, J. Therm. Spray Technol. 2011, 20, 534.
- [27] G. Mauer, J. Therm. Spray Technol. 2019, 28, 27.
- [28] M. Jadidi, M. Mousavi, S. Moghtadernejad, A. Dolatabadi, J. Therm. Spray Technol. 2015, 24, 11.
- [29] M. Jadidi, A. Z. Yeganeh, A. Dolatabadi, J. Therm. Spray Technol. 2018,
- [30] K. VanEvery, M. J. M. Krane, R. W. Trice, H. Wang, W. Porter, M. Besser, D. Sordelet, J. Ilavsky, J. Almer, J. Therm. Spray Technol. **2011**, 20, 817.



www.advancedsciencenews.com

www.aem-journal.com

- [31] a) P. Sokołowski, S. Kozerski, L. Pawłowski, A. Ambroziak, Surf. Coat. Technol. 2014, 260, 97; b) P. Sokołowski, L. Pawłowski, D. Dietrich, T. Lampke, D. Jech, J. Therm. Spray Technol. 2016, 25, 94.
- [32] B. Bernard, A. Quet, L. Bianchi, V. Schick, A. Joulia, A. Malié, B. Rémy, J. Therm. Spray Technol. 2017, 26, 1025.
- [33] R. C. Seshadri, G. Dwivedi, V. Viswanathan, S. Sampath, J. Therm. Spray Technol. 2016, 25, 1666.
- [34] O. Racek, J. Therm. Spray Technol. 2010, 19, 841.
- [35] M. Gupta, N. Markocsan, X.-H. Li, L. Östergren, J. Therm. Spray Technol. 2018, 27, 84.
- [36] Y. Zhao, Z. Yu, M.-P. Planche, A. Lasalle, A. Allimant, G. Montavon, H. Liao, J. Therm. Spray Technol. 2018, 27, 73.
- [37] G. Mauer, M. Gindrat, M. F. Smith, J. Therm. Spray Technol. 2016, 25, 1383.
- [38] W. He, G. Mauer, M. Gindrat, R. Wäger, R. Vaßen, J. Therm. Spray Technol. 2016, 26, 83.
- [39] D. Zhou, O. Guillon, R. Vaßen, Coatings 2017, 7, 120.
- [40] P. Wang, W. He, G. Mauer, R. Mücke, R. Vaßen, Surf. Coat. Technol. 2018, 335, 188.
- [41] G. Mauer, A. Hospach, N. Zotov, R. Vaßen, J. Therm. Spray Technol. 2013, 22, 83.
- [42] W. He, G. Mauer, A. Schwedt, O. Guillon, R. Vaßen, J. Eur. Ceram. Soc. 2018, 38, 2449.

- [43] U. Schulz, M. Schmücker, Mater. Sci. Eng., A 2000, 276, 1.
- [44] S. Rezanka, C. Somsen, G. Eggeler, G. Mauer, R. Vaßen, O. Guillon, Plasma Chem. Plasma Process. 2018, 38, 791.
- [45] F. Traeger, K.-H. Rauwald, R. Vaßen, D. Stöver, Adv. Eng. Mater. 2003, 5, 429.
- [46] D. Zhou, J. Malzbender, Y. J. Sohn, O. Guillon, R. Vaßen, J. Eur. Ceram. Soc. 2019, 39, 482.
- [47] D. Zhou, D. E. Mack, P. Gerald, O. Guillon, R. Vaßen, Ceram. Int. 2019, 45, 18471.
- [48] D. Zhou, Columnar Structured Thermal Barrier Coatings Deposited by Axial Suspension Plasma Spraying [E-Book], Forschungszentrum, Zentralbibliothek, Jülich 2019.
- [49] D. Zhou, D. E. Mack, E. Bakan, G. Mauer, D. Sebold, O. Guillon, R. Vaßen, J. Am. Ceram. Soc. 2019, https://doi.org/10.1111/jace. 16862
- [50] S. Rezanka, G. Mauer, R. Vaßen, J. Therm. Spray Technol. 2014, 23, 182.
- [51] G. Mauer, M. O. Jarligo, D. Marcano, S. Rezanka, D. Zhou, R. Vaßen, IOP Conf. Ser.: Mater. Sci. Eng. 2017, 181, 012001.
- [52] S. Rezanka, D. E. Mack, G. Mauer, D. Sebold, O. Guillon, R. Vaßen, Surf. Coat. Technol. 2017, 324, 222.
- [53] R. Vaßen, A. Stuke, D. Stöver, J. Therm. Spray Technol. 2009, 18, 181.